Inorganica Chimica Acta 363 (2010) 3070–3077

Contents lists available at ScienceDirect

Inorganica Chimica Acta

journal homepage: www.elsevier.com/locate/ica

Organoosmium complexes of imidazole-containing chelate acceptor ligands

Orkan Sarper [a], Biprajit Sarkar [a], Jan Fiedler [b], Falk Lissner [a], Wolfgang Kaim [a,*]

[a] Institut für Anorganische Chemie, Universität Stuttgart, Pfaffenwaldring 55, D-70550 Stuttgart, Germany
[b] J. Heyrovský Institute of Physical Chemistry, v.v.i., Academy of Sciences of the Czech Republic, Dolejškova 3, CZ-18223 Prague, Czech Republic

ARTICLE INFO

Article history:
Received 5 February 2010
Received in revised form 1 April 2010
Accepted 6 April 2010
Available online 11 April 2010

Dedicated to Animesh Chakravorty

Keywords:
Arene ligand
Electrochemistry
Electronic structure
Imidazole ligands
Osmium complexes

ABSTRACT

The complexes $[(L)Os(\eta^6\text{-Cym})Cl](PF_6)$, Cym = *p*-cymene and L = bis(1-methylimidazol-2-yl)ketone (bik) or bis(1-methylimidazol-2-yl)glyoxal (big), were obtained and characterized with respect to spectroscopy, crystal structure (big complex) and (spectro)electrochemical behaviour at variable temperatures. DFT calculations confirm the structure of $[(big)Os(\eta^6\text{-Cym})Cl]^+$ with imidazolyl-N-bonded Os^{II} in a boat-shaped seven-membered chelate ring with small N–Os–N angles (<84°). Reduction of this compound proceeds reversibly to a neutral complex of the α-semidione radical anion ligand $big^{\cdot-}$; EPR and IR spectroelectrochemistry indicate very little participation from the heavy metal in the spin distribution. The analogous $[(bik)Os(\eta^6\text{-Cym})Cl]^+$ could not be reduced reversibly to the ketyl radical complex but displayed a more reversible oxidation at high potential.

© 2010 Elsevier B.V. All rights reserved.

1. Introduction

Histidine-bound metal centers are frequently encountered in bioactive sites of proteins [1]. Thus, many bio-inspired imidazole-containing ligands have been synthesized and studied [2,3]. The purpose of these ligands is not limited to the modelling of metalloprotein active sites [4], they have also been investigated in the context of asymmetric catalysis and for the separation and detection of biomolecules [5].

Bis(1-methylimidazol-2-yl)ketone (bik) [6] and bis(1-methylimidazol-2-yl)glyoxal (big) [7–9] as examples for carbonyl-bridged imidazole-containing ligands were studied previously in combination with various metal centers such as Pt^{II}, Cu^{I}, Cu^{II}, Ru^{II}, W^{VI}, Ir^{III}, Rh^{III}, Au^{III}, Re^{I} [3,8,9,11] and, most recently, with Pt^{IV} [10]. Electrochemical investigations were performed on these species.

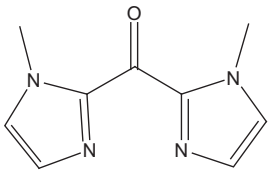

bik

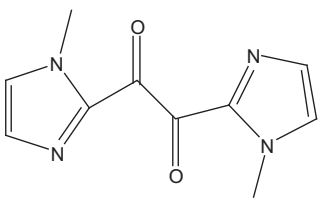

big

Based on the DFT calculations and on electrochemical results, the ligand big in the co-planar conformation (which has a low lying π^* orbital on the α-diketo moiety) is more easily reduced than bik [10,11]. π Back donation to the metal center is observed in such complexes due to the existence of the extra carbonyl fragment. Recent DFT studies on big and on its Au^{III}, Pt^{II}, Cu^{II}, Re^{I} and Zn^{II} complexes showed that it coordinates by transferring charge to the metal via the imidazole N atoms while the low lying unoccupied π^* orbital can overlap with filled d orbitals of the metal [11].

The ligand big, having four binding atom sites, is a potential tetradentate π acceptor ligand. Thus, it has the possibility to form mono- and di-nuclear metal complexes [9a]. The possible coordination of metal ions by the oxygen atoms or by the imidazole nitrogen centers can result in mononuclear complexes [3,8] while coordination through all oxygen and nitrogen atoms may occur in a di-nuclear fashion, forming either five- or six-membered chelate rings (Scheme 1) [9].

There has also been great interest in the homogenous catalysis of hydride transfer reactions during the last decades [12]. Such reactions are useful for the generation of fuels (e.g. H_2 from H^+) or for the regeneration of NADH from NAD^+ in biotechnological processes [13]. In attempts to modify existing [12,13] catalysts, various transition metal moieties with C_nR_n co-ligands in combination with imine-nitrogen containing ligands have been used. Cp^* (pentamethylcyclopentadienyl) which was used in the cases of $[M(L)(C_5R_5)X]^+$, M = Ir^{III} or Rh^{III}, has also been replaced by *p*-cymene (Cym) or hexamethylbenzene in $[M(L)(C_6R_6)X]^+$ when the metal was changed to Ru^{II} or Os^{II} [12e,14].

* Corresponding author.
E-mail address: kaim@iac.uni-stuttgart.de (W. Kaim).

0020-1693/$ - see front matter © 2010 Elsevier B.V. All rights reserved.
doi:10.1016/j.ica.2010.04.007

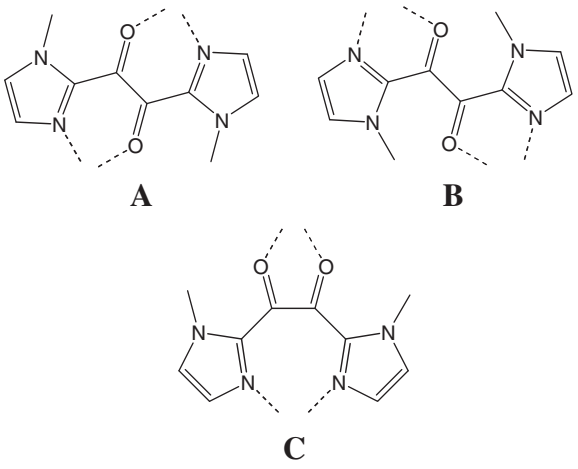

Scheme 1. Alternative coordination possibilities for bis-chelate complexes of big.

This contribution presents the syntheses, characterization, EPR and spectroelectrochemical studies of mononuclear Os^{II} complexes [(big)Os(Cym)Cl](PF_6) and [(bik)Os(Cym)Cl](PF_6) with the ligands big and bik. The molecular and crystal structure of [(big)Os(Cym)Cl](PF_6) will be discussed.

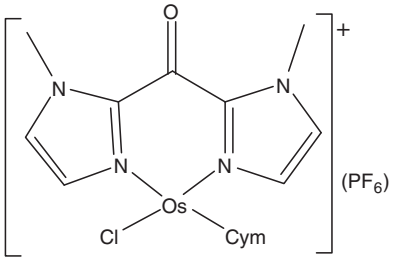

[(bik)Os(Cym)Cl](PF_6)

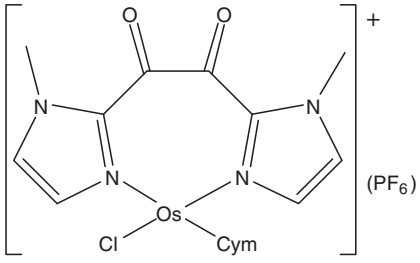

[(big)Os(Cym)Cl](PF_6)

2. Results and discussion

2.1. Syntheses

While bik was prepared in accordance with the literature [6a,d], the ligand big was obtained by reacting 1-methylimidazole with a slight excess of *n*-butyllithium at −70 °C [7–9] in THF, followed by addition of oxalyl chloride.

Both mononuclear complexes were synthesized by the reaction of one equivalent of $[Os(Cym)Cl_2]_2$ with two equivalents of the respective ligand in acetonitrile under argon. Due to the heat sensitivity of big, [(big)Os(Cym)Cl](PF_6) was synthesized at 60 °C whereas [(bik)Os(Cym)Cl](PF_6) was prepared at reflux conditions. In order to substitute the Cl^- counter ion, $NH_4(PF_6)$ was added, which resulted in the precipitation of the PF_6 salts. The addition of excess amounts of $[Os(Cym)Cl_2]_2$ did not yield any di-nuclear complexes even after prolonged reaction, as confirmed by ^1H NMR spectroscopy.

2.2. ^1H NMR spectroscopy

Changes in the positions of the aromatic ring hydrogen and N-methyl ^1H NMR signals compared to the free bik and big ligands, and the changes in the cymene protons' signals with respect to the precursor $[Os(Cym)Cl_2]_2$ indicate the formation of [(bik)-Os(Cym)Cl](PF_6) and [(big)Os(Cym)Cl](PF_6).

All proton signals of the imidazole rings, including the methyl protons, shift downfield in [(bik)Os(Cym)Cl](PF_6) with respect to free bik (Table 1). In contrast, the proton signals on the cymene ligand shift upfield relative to the precursor.

On complexation, one pair of imidazole–H signals of big in the aromatic region shows an upfield shift, whereas the other pair is downfield shifted compared to the free ligand. The downfield shifted proton signals can be assigned to H_4 and $H_{4'}$ due to the proximity to the metal coordination site. Methyl proton resonances for the imidazole rings shift similarly downfield with respect to free big. On the other hand, complexation of big results in an upfield shift of the cymene proton signals when compared to the dimeric precursor.

2.3. Infrared spectroscopy

IR spectral analyses of [(bik)Os(Cym)Cl](PF_6) and [(big)Os-(Cym)Cl](PF_6) in the solid state show sharp absorption bands of $\nu_{C=O}$ (1648 and 1673 cm^{-1}, respectively), shifted to higher wavenumbers in comparison the free ligands (Table 2). Similarly, the IR carbonyl frequency in [(bik)$AuCl_2$]Cl (1689 cm^{-1}) [3] appears at higher energy when compared to the carbonyl stretching band of bik (1637 cm^{-1}). The reported DFT calculated HOMO of big

Table 1
^1H NMR chemical shifts from $CDCl_3$ solutions.

Compound	Cymene-H				Imidazole-H	
	Aromatic (m)	*i*-Pr-CH_3(d)	CH_3(s)	*i*-Pr-H(sept)	Im-H(d)	N-CH_3(s)
$[Os(Cym)Cl_2]_2$	6.01; 6.19	1.26; 1.30	2.21	2.79	–	–
big	–	–	–	–	7.14; 7.25	4.14
[(big)Os(Cym)Cl](PF_6)	5.36; 5.65	1.12	1.63	2.26	6.92; 7.31	4.21
bik	–	–	–	–	7.15; 7.35	4.05
[(bik)Os(Cym)Cl](PF_6)	5.78; 5.90	1.19	2.21	–	7.35; 7.60	4.25

Table 2
CO stretching frequencies from IR spectroscopy.[a]

Compound	ν(C=O) (cm^{-1})
bik	1637
big	1662
[(bik)Os(Cym)Cl](PF_6)	1648
[(big)Os(Cym)Cl](PF_6)	1673

[a] In KBr.

shows anti-bonding character over the carbonyl system [11]. Electron density shift from that orbital to the metal center upon complexation increases the carbonyl bond order.

2.4. UV–Vis spectroscopy

The complex [(bik)Os(Cym)Cl](PF_6) shows an intense absorption in CH_2Cl_2 solution at 331 nm (ε = 13 100 $M^{-1}cm^{-1}$) and a less intense band at 415 nm (ε = 1890 $M^{-1}cm^{-1}$). There are also shoulders at 318, 358 and 374 nm. The UV–Vis spectrum of [(big)Os(Cym)Cl](PF_6) in dry CH_2Cl_2 exhibits an intense absorption at 320 nm (ε = 21 700 $M^{-1}cm^{-1}$) and a shoulder at 420 nm. The bands at 330 nm may be assigned to π–π^* transitions. A similar absorption for Pt(big)Cl_2 was reported at 318 nm in CH_2Cl_2 [9b]. The absorption around 420 nm is tentatively attributed to an MLCT transition which was encountered similarly in related Os^{II} complexes [12d]. Both complexes are not light sensitive.

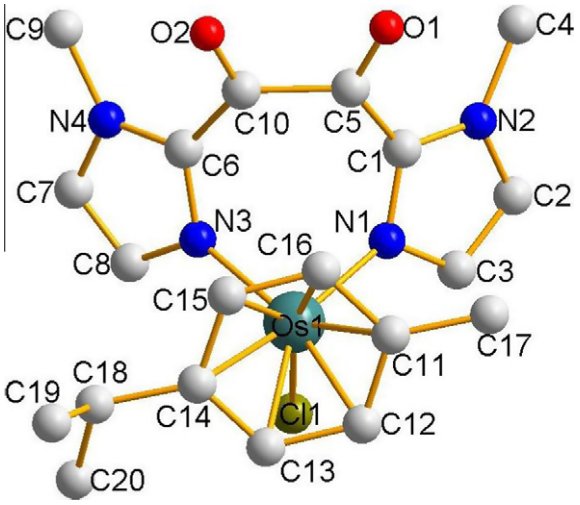

Fig. 1. One of the crystallographically independent molecular ions [(big)Os(Cym)Cl]$^+$ in the crystal of the hexafluorophosphate.

2.5. Structural investigation of [(big)Os(Cym)Cl](PF_6)

Orange crystals suitable for X-ray diffraction were obtained by slow diffusion of *n*-hexane into a CH_2Cl_2 solution of [(big)Os(Cym)Cl](PF_6) at −20 °C. The complex crystallizes in the monoclinic

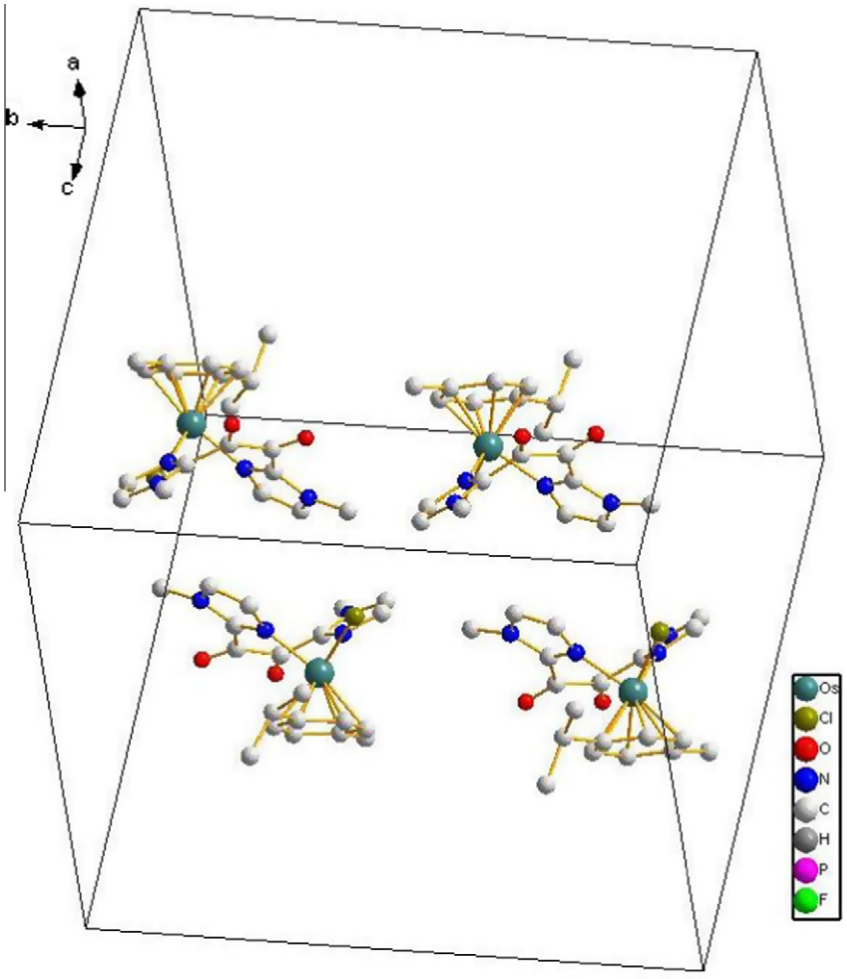

Fig. 2. Arrangement of four crystallographically different [(big)Os(Cym)Cl]$^+$ ions in the unit cell of the hexafluorophosphate.

Table 3
Selected bond distances (Å) for [(big)Os(Cym)Cl](PF$_6$) (Exp.)[a] and [(big)Os(C$_6$H$_6$)Cl]$^+$ (DFT).

Bond	Exp.[a]	DFT[b]
Os–N	2.095	2.127
Os–Cl	2.397	2.421
Os–C(Cym)	2.192	2.240
C=O	1.209	1.216
(O)C–C(O)	1.56	1.570

[a] Average values for four independent molecules in the crystal.
[b] [(big)Os(C$_6$H$_6$)Cl]$^+$ calculated by DFT.

Table 4
Selected angles (°) of [(big)Os(Cym)Cl](PF$_6$).[a,b]

Angles	Exp.	DFT[b]	Torsional angles	Exp.	DFT[b]
N–Os–N	83.4	83.1	Os–N–C–C	8.7	7.7
N–Os–Cl	85.2	85.6	O–C–C–N	33.2	31.4
Im–Im′ [b,c]	66.9	65.7	O–C–C–O	1.1	0.8

[a] Exp.: average values for four independent molecules.
[b] DFT: for [(big)Os(C$_6$H$_6$)Cl]$^+$.
[c] Dihedral angle between methyl-imidazole planes.

space group *Pc*. The crystal contains four structurally similar but crystallographically independent molecules of [(big)Os(Cym)Cl](PF$_6$) which are presented in Figs. 1 and 2. The experimentally determined (average) bond lengths for the complex monocation and the DFT values obtained for the cationic and singly reduced (neutral) radical complex [(big)Os(C$_6$H$_6$)Cl]· are given in Table 3. Table 4 shows the measured and calculated bond and dihedral angles (averaged values). Further details of the crystallographic parameters are given in Section 3.

The X-ray structural analysis of the four independent molecules reveals N,N'-coordination of the ligand, forming seven-membered chelate rings with a boat conformation, as was previously found for PtCl$_2$(big) [9b], [(big)RhCp*Cl](PF$_6$) [8] and *fac*-(big)Re(CO)$_3$Cl [9a]. The metal is surrounded by a η^6-coordinated cymene co-ligand, one chloride, and two nitrogen atoms from the ligand big in a quasi-hexacoordinated fashion. The α-diketo group of the ligand becomes almost co-planar upon complexation.

The presence of η^6-cymene at Os causes asymmetry of the complex. Thus, the two halves of the big ligand in the complex are not symmetrical, unlike in the previously reported complexes of big [8,9]. The Os–N bonds on the side of the methyl group of cymene are ranging from 2.035(16) to 2.149(14) Å, whereas the Os–N bonds on the other side vary only between 2.081(12) and 2.102(12) Å.

The N–Os–N angles for the four crystallographically different Os centers vary from 82.9(5)° to 83.9(5)°. These angles are remarkably smaller than the previously reported bite angles of 91.2(3)° for Re(CO)$_3$Cl(big) [9a], 88.37(18)° for [Cp*Cl(big)Rh](PF$_6$) [8], 89.(2)° for PtCl$_2$(big) [9b] and 87.01(3)° for Pt(CH$_3$)$_3$I(big) [10]. DFT calculations confirm the small angle (83.1°) for the model cation [(big)Os(C$_6$H$_6$)Cl]$^+$.

The dihedral angles between both imidazole planes in each of the four different molecules (Im1–Im1′, etc.) vary from 64.9° to 69. 6°, similar to reported values [8–10]. The free ligand adopts a structure where two halves of the molecule are perpendicular to each other [8]. Upon complexation, the imidazole rings together with the α-diketo moiety do not completely planarize although there is a significant change from the perpendicular arrangement. Thus, the O(C)–(C′)–O′ dihedral angle which was 88.5° for free big diminishes, ranging from −3.4° to 8.1° in the Os^{II} complex molecules in the crystal; it is calculated to be 0.78° by DFT for [(big)Os[(C$_6$H$_6$)Cl]$^+$.

Intra-carbonyl bond distances in the complex appear within a range from 1.19(2) to 1.24(2) Å for that half of big on the cymene-methyl side, whereas the C–O bond lengths in the cymene-isopropyl vicinity are between 1.194(18) and 1.214(17) Å. The average C=O bond length of the complex (1.209 Å) is slightly shorter than the carbonyl bond distance reported for free big (1.216(2) Å) which is in agreement with the high-energy shift of the carbonyl band observed in the IR spectrum upon complexation.

The C–C bond lengths in the α-diketo moiety vary between 1.54(2) and 1.58(2) Å which is only slightly longer than the value of free big of 1.542(2) Å. Carbonyl bond shortening and C–C′ bond elongation can be explained by the DFT calculated HOMO of big [11] (see also Fig. 6). It shows the characteristics of an anti-bonding molecular orbital with regard to the two carbonyl groups, and characteristics of a bonding molecular orbital as concerns the C–C′ bond. By electron donation from the HOMO to the Os metal center upon complexation, the bonding character of C=O increases, causing shortening (increasing bond order).

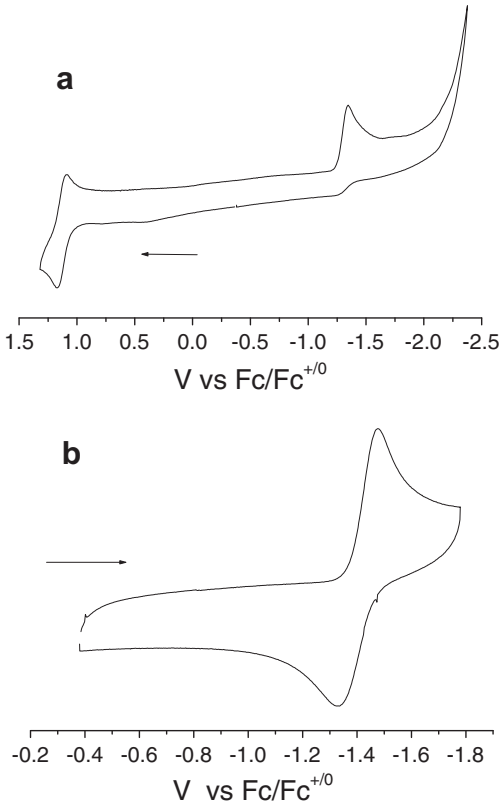

Fig. 3. Cyclic voltammograms of [(bik)Os(Cym)Cl](PF$_6$) in CH$_2$Cl$_2$/0.1 M Bu$_4$NPF$_6$ (a) at 25 °C, scan rate 100 mV/s and (b) at −50 °C, scan rate 500 mV/s.

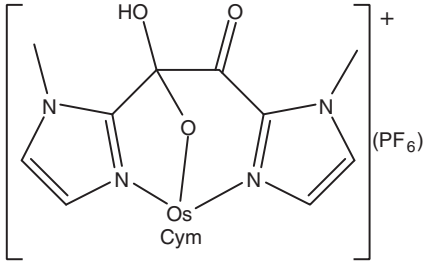

Scheme 2. Assumed structure of [(bigOH)Os(Cym)](PF$_6$).

A previously reported $[Cp^*Ir]^{2+}$ complex of big reacted with water to yield structurally characterized [(bigOH)IrCp*](PF6) in which the metal center is coordinated to the C-addition product bigOH through two nitrogen atoms and one negatively charged oxygen, as revealed by the crystal structure analysis [8]. During crystallization of [(big)Os(Cym)Cl](PF6), additional yellow crystals were obtained. X-ray structural analysis of those yellow crystals suggest the formation of [(bigOH)Os(Cym)](PF6) (Scheme 2) but unfortunately with poor crystal quality. Apparently, residual water in the solvent reacted with [(big)Os(Cym)Cl](PF6) during the crystallization to yield this bridged single carbonyl structure, as in the case of the Ir^{III} analogue, reflecting strong polarizing effects from Os^{II} and Ir^{III}.

2.6. Electrochemistry

At room temperature, the complex [(bik)Os(Cym)Cl](PF6) is reduced irreversibly at a cathodic peak potential of −1.35 V versus $Fc^{+/0}$ in CH_2Cl_2/0.1 M Bu_4NPF_6. The reduction wave becomes partially reversible only at −50 °C with a half-wave potential of −1.40 V. The ratio of anodic current to cathodic current, I_{Pa}/I_{Pc}, remains below 1.0 at a scan rate of 500 mV/s, illustrating the incompletely reversible character of the reduction.

As supported by DFT and infrared spectroelectrochemistry studies, the reduction at −1.35 V occurs on the C=O group, causing the formation of a ketyl-type radical. The facilitated reduction of the bik complex in relation to the free ligand (−2.25 V) illustrates the polarization of the ligand π system through metal coordination [8].

On the anodic side of the cyclic voltammogram of $[(bik)Os(Cym)Cl]^+$, a reversible oxidation with a half-wave potential of 1.13 V is observed at room temperature (Fig. 3 and Table 5). This oxidation wave can be assigned to a metal-centered process, a reversible oxidation from Os^{II} to Os^{III}.

The cationic complex ion [(big)Os(Cym)Cl](PF6) can be reversibly reduced at room temperature with a half-wave potential of −0.69 V versus $Fc^{+/0}$ in CH_2Cl_2/0.1 M Bu_4NPF_6. In relation to the free ligand (−1.66 V), the facile reduction of the complex illustrates the polarization of the ligand π system through metal coordination. A similar trend was observed for *fac*-$Re(CO)_3Cl$(big) where the reduction potential is −0.95 V in CH_2Cl_2/0.1 M Bu_4NPF_6 [8]. Fig. 4a shows the cyclic voltammogram of the complex in the cathodic region. There is no further reduction observed until −2.0 V.

Previously reported areneosmium(II) complexes show oxidations around 1 V which were assigned as metal-centered processes (Os^{II} to Os^{III}) [12d,14]. For example, [(bpy)OsCl(Cym)](PF6) is oxidized reversibly at 1.12 V and [(bpy)Os(C_6Me_6)Cl](PF6) is oxidized at 0.89 V. For the complex $[(big)Os(Cym)Cl]^+$ of big an irreversible oxidation at 1.19 V at room temperature is observed which sustained its character even at -50 °C at 100 mV/s scan rate. The oxi-

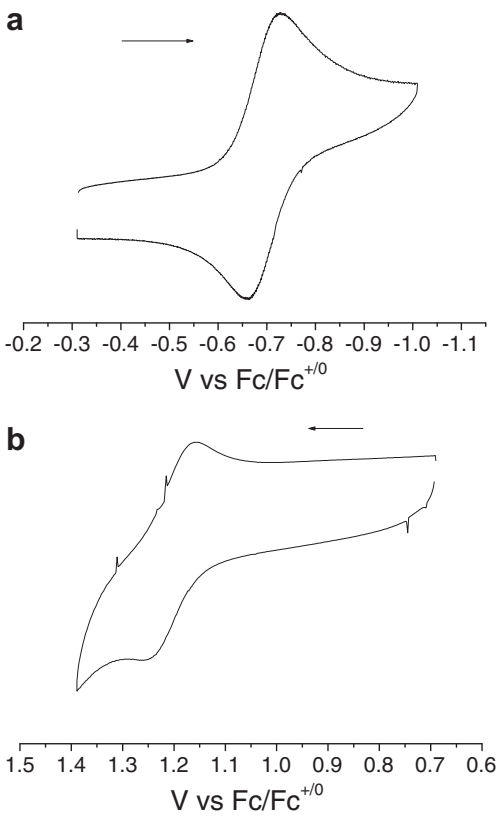

Fig. 4. Cyclic voltammograms of [(big)Os(Cym)Cl](PF6) in CH_2Cl_2/0.1 M Bu_4NPF_6 (a) at 25 °C with a scan rate of 100 mV/s and (b) at −50 °C with a scan rate of 1000 mV/s.

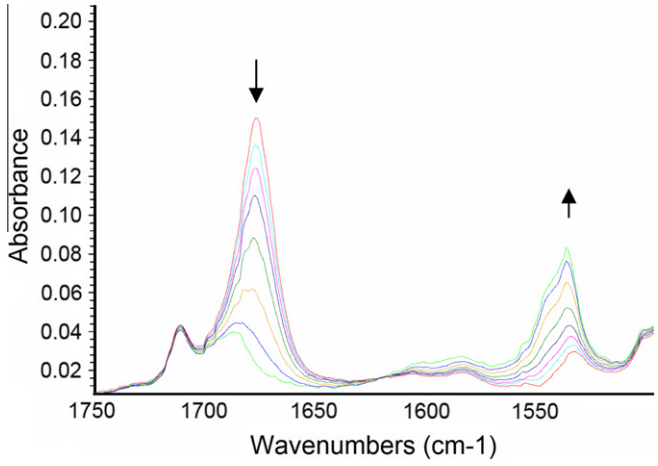

Fig. 5. IR Spectroelectrochemical reduction of [(big)Os(Cym)Cl]PF_6 at 25 °C in CH_2Cl_2/0.1 M Bu_4NPF_6.

Table 5
Electrochemical data of big and bik ligands and of their complexes.[a]

Compound	$E_{1/2}$ (oxidation)	$E_{1/2}$ (reduction)
bik[b]	–	−2.25 (80 mV)
[(bik)Os(Cym)Cl](PF6)	1.13 (80 mV)[c]	−1.40 (70 mV)[d]
big[e]	–	−1.66 (116 mV)
[(big)Os(Cym)Cl](PF6)	1.19 (90 mV)[f]	−0.69 (70 mV)[c]

[a] In V vs. $Fc^{+/o}$.
[b] In DMF.
[c] In CH_2Cl_2/0.1 M Bu_4NPF_6 at 25 °C with a scan rate of 100 mV/s.
[d] In CH_2Cl_2/0.1 M Bu_4NPF_6 at −50 °C with a scan rate of 500 mV/s.
[e] In CH_3CN/0.1 M Bu_4NPF_6 with a scan rate of 100 mV/s.
[f] In CH_2Cl_2/0.1 M Bu_4NPF_6 at −50 °C with a scan rate of 1000 mV/s.

Table 6
IR spectroelectrochemical data.[a]

Compound	ν(C=O) (cm^{-1})
big	1675
big^-	1404
[(big)Os(Cym)Cl]·	1537
[(big)Os(Cym)Cl](PF6)	1678

[a] Measured in CH_2Cl_2/0.1 M Bu_4NPF_6 at room temperature.

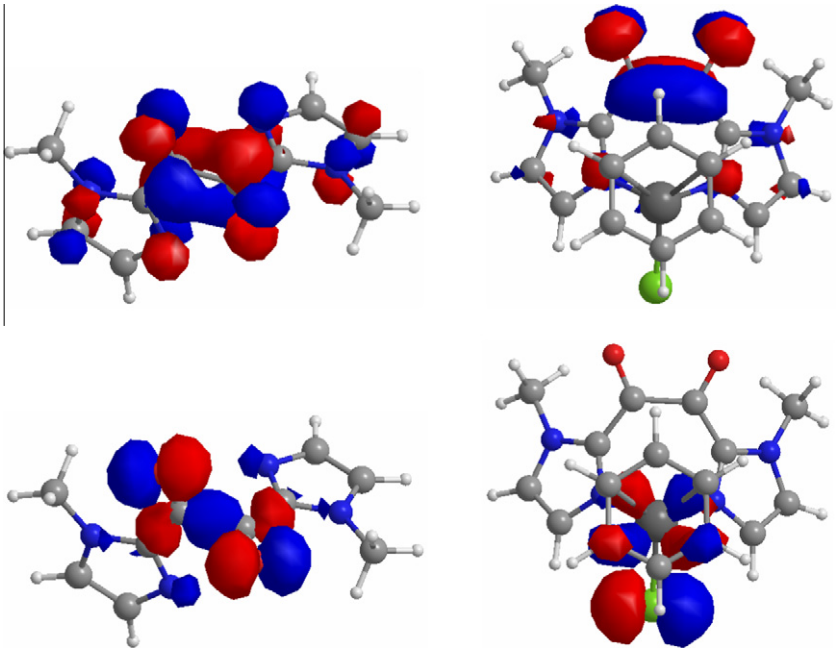

Fig. 6. DFT-calculated LUMOs (top) and HOMOs (bottom) of big (left) and $[(big)Os(C_6H_6)Cl]^+$ (right).

dation, presumably of the metal center, becomes reversible only at a high scan rate of 1000 mV/s at −50 °C (Fig. 4b).

2.7. IR spectroelectrochemistry

With the help of an OTTLE cell [15] the carbonyl stretching bands of the ligands bik and big in the cationic Os^{II} complexes were monitored during the electron transfer processes through IR spectroelectrochemistry.

IR spectroelectrochemical reduction of $[(bik)Os(Cym)Cl](PF_6)$ was performed in CH_2Cl_2 at −60 °C. The CO band diminished at 1646 cm^{-1} but did not reappear at lower wavenumbers, the experiment showed no sign of reversibility which is in agreement with the formation of a labile ketyl-type radical complex.

IR spectroelectrochemistry of $[(big)Os(Cym)Cl](PF_6)$ was carried out in CH_2Cl_2 solution at room temperature. The carbonyl band of the complex at 1678 cm^{-1} shifts reversibly on reduction (Fig. 5 and Table 6) and a new band appears at 1537 cm^{-1}. This lowering of ν_{CO} indicates that the added electron is accumulated on the α-diketone moiety where the ligand has its LUMO [11] (Fig. 6), resulting in the formation of an α-semidione complex (Scheme 3).

2.8. EPR spectroelectrochemistry

The reversible reduction of $[(big)Os(Cym)Cl](PF_6)$ as observed by cyclic voltammetry allowed us to obtain EPR information for the electrochemically generated neutral radical $[(big)Os(Cym)Cl]^{\cdot}$.

In situ electrolysis at room temperature in CH_2Cl_2/0.1 M Bu_4NPF_6 yielded a resolved EPR signal (Fig. 7) at g_{iso} = 2.0073, i.e. reasonably close to the free electron value of g = 2.0023 and to the g factor of $big^{\cdot-}$ (g_{iso} = 2.0054), which supports the idea of a ligand-based reduction. The good resolution of the spectrum allowed us to obtain information from the hyperfine interaction of the involved atoms using computer simulation. The major contributions are from four nitrogen atoms on the big ligand with hyperfine coupling constants of 2 (^{14}N) with a = 2.4 G and 2 (^{14}N) with a = 0.8 G. Hyperfine coupling constants of the imidazole protons are within the linewidth (0.6 G) and are not observed. The hyperfine splitting pattern compares well with the results for $big^{\cdot-}$ [8,9]. Low-temperature EPR measurements (Fig. 8) yielded a slightly anisotropic spectrum with g tensor components of g_1 = 2.0184 and $g_2 = g_3$ = 2.0032.

The narrow EPR spectrum, the small g anisotropy, and the g_{iso} value close to that of the free electron confirm that the single electron is concentrated on the "big" ligand on reduction of the complex, very little contribution occurs from the osmium center with its high spin–orbit coupling constant and a potentially EPR-active [12d] ^{189}Os isotope (I = 3/2, 16.1%). Experimental and simulated

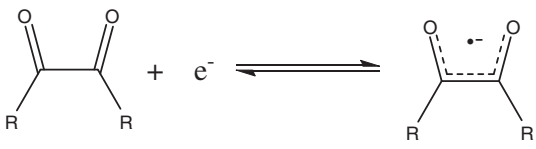

Scheme 3. Formation of an α-semidione by one-electron reduction (*syn*-configuration).

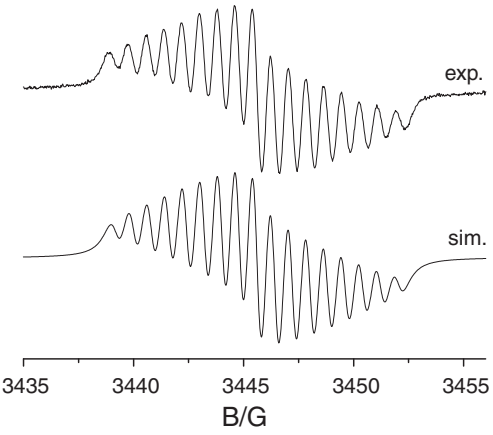

Fig. 7. EPR spectrum of $[(big)Os(Cym)Cl]^{\cdot}$ in CH_2Cl_2/0.1 M Bu_4NPF_6 at 25 °C with simulated signal: 2 (^{14}N), a = 2.4 G and 2 (^{14}N), a = 0.8 G.

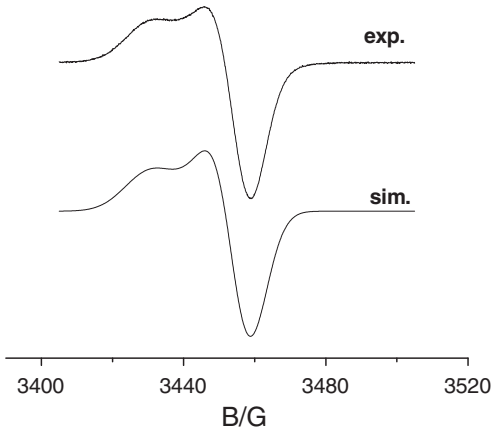

Fig. 8. EPR spectrum of [(big)Os(Cym)Cl]· in CH_2Cl_2/0.1 M Bu_4NPF_6 at 110 K with simulated signal, $g_1 = 2.0184$ and $g_2 = g_3 = 2.0032$.

spectra are given in Figs. 7 and 8, DFG calculations confirm the ligand-based LUMO of the precursor (Fig. 6).

2.9. Conclusion

While both osmium complexes [(L)Os(Cym)Cl](PF_6), L = bik or big, have the metal bound by the imidazole imine donor atoms of L as evident from structure analysis (big complex) and ^{1}H NMR spectroscopy, the superior electron transfer capability of the ligand big with the α-diketo function as electro-active group results in a pronounced stabilization of the reduced form, the spectroelectrochemically characterized neutral semidione radical complex [(big)Os(Cym)Cl]·.

3. Experimental

3.1. Materials and techniques

EPR spectra in the X band were recorded with a Bruker System EMX. ^{1}H NMR spectra were taken on a Bruker AC 250 spectrometer. IR spectra were obtained using a Nicolet 6700 FT-IR instrument; solid state IR measurements were performed with an ATR unit (smart orbit with diamond crystal). UV–Vis–NIR absorption spectra were recorded on J&M TIDAS and Shimadzu UV 3101 PC spectrophotometers. Cyclic voltammetry was carried out in 0.1 M Bu_4NPF_6 solutions using a three-electrode configuration (glassy carbon working electrode, Pt counter electrode, Ag/AgCl reference) and a PAR 273 potentiostat and function generator. The ferrocene/ferrocenium (Fc/Fc^+) couple served as internal reference. Spectroelectrochemistry was performed using an optically transparent thin-layer electrode (OTTLE) cell [15]. A two-electrode capillary served to generate intermediates for X band EPR studies.

3.2. Syntheses

3.2.1. Synthesis of [(bik)Os(Cym)Cl](PF$_6$)

A mixture containing 100 mg (0.126 mmol) of $[Os(Cym)Cl_2]_2$ and 48 mg (0.252 mmol) bik in 40 ml acetonitrile was heated to reflux under an argon atmosphere for 10 h. After cooling, the solvent was removed under reduced pressure until about 10 ml was left. A concentrated solution of 200 mg ammonium hexafluorophosphate in acetonitrile was added. This solution was left at 0 °C overnight, filtered and dissolved in CH_2Cl_2. The yellow-orange solution was then filtered to remove the precipitated NH_4Cl. Evaporation of the solvent under vacuum gave an orange-yellow powder. Yield: 90 mg (0.130 mmol, 51%). *Anal.* Calc. for $C_{19}H_{24}ClF_6N_4POOs$ (695.05 g/mol): C, 32.83, H, 3.48, N, 8.06. Found: C, 32.80, H, 3.52, N, 7.87%. ^{1}H NMR ($CDCl_3$): $\delta = 1.19$ (d, $^3J = 6.9$ Hz, 6H), 2.21 (s, 3H), 2.64 (sept, 1H), 4.25 (s, 6H), 5.78 (m, 2H), 5.90 (m, 2H), 7.35 (m, 2H), 7.60 (m, 2H). IR (solid): 1648 cm^{-1} ($\nu_{C=O}$). UV/Vis (CH_2Cl_2): λ_{max}/nm (ε/M^{-1} cm^{-1}) = 415(1890), 372(sh), 357(sh), 331(13 100). Mass spectroscopy: 551.12 (*m*/*z* calculated for M−PF_6^-); 551.12 (*m*/*z* observed).

3.2.2. Synthesis of [(big)Os(Cym)Cl](PF$_6$)

A mixture containing 100 mg (0.126 mmol)) $[Os(Cym)Cl_2]_2$ and 55 mg (0.252 mmol) of big in 40 ml acetonitrile was stirred at 60 °C under an argon atmosphere for 24 h. After cooling, the solvent was removed under reduced pressure until about 10 ml was left. A concentrated solution of 200 mg ammonium hexafluorophosphate in acetonitrile was added. This solution was left at 0 °C overnight, filtered and dissolved in CH_2Cl_2. The red-orange solution was again filtered to remove precipitated NH_4Cl. Evaporation of the solvent under vacuum gave the orange main product and a very small amount of yellow side product, tentatively identified as [(bigOH)Os(Cym)](PF_6) by X-ray crystallography (see text). Yield: 55 mg (0.077 mmol, 30%). *Anal.* Calc. for $C_{20}H_{24}ClF_6N_4PO_2Os$ (723.06 g/mol): C, 33.22, H, 3.35, N, 7.75. Found: C, 33.35, H, 3.57, N, 7.08%. ^{1}H NMR ($CDCl_3$): $\delta = 1.12$ (d, $^3J = 6.9$ Hz, 6H), 1.63 (s, 3H), 2.27 (m, 1H), 4.21 (s, 6H), 5.37 (d, $^3J = 5.6$ Hz, 2H), 5.66 (d, $^3J = 5.6$ Hz, 2H), 6.92 (d, $^3J = 2.9$ Hz, 2H), 7.31 (d, $^3J = 2.9$ Hz, 2H). IR (solid): 1673 cm^{-1} ($\nu_{C=O}$). UV/Vis (CH_2Cl_2): λ_{max}/nm (ε/M^{-1} cm^{-1}) = 436(sh), 324, 278(sh). Mass spectroscopy: 575.17 (*m*/*z* calculated for M−PF_6^-, M−Cl^-, M+CH_3O^- from methanol solvent); 575.17 (*m*/*z* observed).

3.3. Crystallography

Orange crystals of [(big)Os(Cym)Cl](PF_6) suitable for X-ray diffraction were obtained by slow diffusion of n-hexane into a CH_2Cl_2 solution at −20 °C. Empirical formula: $C_{20}H_{24}ClF_6N_4O_2OsP$; formula weight: 723.06 g mol^{-1}; temperature = 100(2) K; wavelength = 0.71073 Å (Mo Kα radiation); crystal system: monoclinic; space group: *Pc*; unit cell dimensions: $a = 15.1557(3)$ Å; $b = 19.5985(5)$ Å; $c = 17.7164(4)$ Å; $\beta = 114.9550(10)°$; $V = 4770.99(19)$ Å^3; $\rho_{calc} = 2.013$ g cm^{-3}; absorption coefficient = 5.598 mm^{-1}; max. $2\theta = 27.88°$; $-19 \leqslant h \leqslant 19$, $-24 \leqslant k \leqslant 25$, $-23 \leqslant l \leqslant 23$; $Z = 8$; reflns.: 20 609, unique reflns.: 20 602; R_{int}/R_σ: 0.0322/0.0840; GOF/F^2: 1.050; data/restraints/parameters: 20 602/2/1107; R (all data): $R_1 = 0.0848$, $wR_2 = 0.1042$; R ($I > 2\sigma(I)$): $R_1 = 0.0519$, $wR_2 = 0.0924$; max./min. res. dens: 2.534, −2.258 e Å^{-3}. Data were collected with a NONIUS Kappa CCD diffractometer at 100 K. The structure was solved using direct methods with refinement by full-matrix least-squares of F^2, employing the program system SHELXL 97 in connection with absorption correction [16]. All non-hydrogen atoms were refined anisotropically, and hydrogen atoms were introduced at appropriate positions. Tables 3 and 4 give averaged structure parameters for comparison with calculations, the individual values are available from the Supplementary material.

3.4. DFT calculations

Density functional (DFT) calculations were carried out using the program package GAUSSIAN '03 [17]. The hybrid functional B3LYP with the 6-31G* basis set for main group elements and MWB for the Os metal was employed. The structure was fully optimized starting from the average geometry obtained from the X-ray diffraction experiment. Benzene was substituted for cymene.

4. Supplementary material

CCDC 765252 contains the supplementary crystallographic data for this paper. These data can be obtained free of charge from The Cambridge Crystallographic Data Centre via http://www.ccdc.cam.ac.uk/data_request/cif.

Acknowledgements

Support from Deutsche Forschungsgemeinschaft, Fonds der Chemischen Industrie (Germany) and COST (European Union) is gratefully acknowledged.

References

[1] (a) W. Kaim, B. Schwederski, Bioinorganic Chemistry, Wiley, Chichester, UK, 1994;
(b)A. Messerschmidt, R. Huber, T. Poulos, K. Wieghardt (Eds.), Handbook of Metalloproteins, Wiley, New York, 2001;
(c)I. Bertini, H. Sigel (Eds.), Handbook on Metalloproteins, Marcel Dekker, New York, 2001.
[2] (a) S.M. Gorun, G.C. Papaefthymiou, R.B. Frankel, S.J. Lippard, J. Am. Chem. Soc. 109 (1987) 4244;
(b) S.M. Gorun, S.J. Lippard, Inorg. Chem. 27 (1988) 149;
(c) W.B. Tolman, A. Bino, S.J. Lippard, J. Am. Chem. Soc. 111 (1989) 8522;
(d) M.J. Bloemink, H. Engelking, S. Karentzopoulos, B. Krebs, J. Reedijk, Inorg. Chem. 35 (1996) 619.
[3] E. Bulak, O. Sarper, A. Dogan, F. Lissner, Th. Schleid, W. Kaim, Polyhedron 25 (2006) 2577.
[4] (a) I. Sovago, K. Varnagy, K. Osz, Comments Inorg. Chem. 23 (2002) 149;
(b) M. Abuskhuna, J. McCann, M. Briody, V. Devereux, S. McKee, Polyhedron 23 (2004) 1731;
(c) T. Ruether, K.J. Cavell, N.C. Braussaud, B.W. Skelton, A.H. White, J. Chem. Soc., Dalton Trans. (2002) 4684;
(d) R. Bhalla, M. Helliwell, R.L. Beddoes, D. Collison, C.D. Garner, Inorg. Chim. Acta 273 (1998) 225.
[5] A. Kumar, I.Y. Galaev, B. Mattiasson, Bioseparation 7 (1998) 185.
[6] (a) P.K. Byers, A.J. Canty, L.M. Engelhardt, J.M. Patrick, A.H. White, J. Chem. Soc., Dalton Trans. (1985) 981;
(b) X.-M. Chen, Z.-T. Xu, T.C.W. Mak, Polyhedron 14 (1995) 319;
(c) M. Grehl, B. Krebs, Inorg. Chem. 33 (1994) 3877;
(d) G. Reusmann, M. Grehl, W. Reckordt, B. Krebs, Z. Anorg. Allg. Chem. 620 (1994) 199;
(e) A.F. Stange, W. Kaim, Z. Anorg. Allg. Chem. 622 (1996) 1118;
(f) M. Koley, B. Sarkar, S. Ghumaan, E. Bulak, J. Fiedler, W. Kaim, G.K. Lahiri, Inorg. Chem. 46 (2007) 3736;
(g) P. De, B. Sarkar, S. Maji, A.K. Das, E. Bulak, S.M. Mobin, W. Kaim, G.K. Lahiri, Eur. J. Inorg. Chem. (2009) 2702;
(h) F.M. Hornung, O. Heilmann, W. Kaim, S. Záliš, J. Fiedler, Inorg. Chem. 39 (2000) 4052.
[7] P. Fournari, P. de Cointet, E. Laviron, Bull. Soc. Chim. Fr. 6 (1968) 2438.
[8] M. Albrecht, W. Kaim, Z. Anorg. Allg. Chem. 626 (2000) 1341.
[9] (a) A. Knödler, M. Wanner, J. Fiedler, W. Kaim, J. Chem. Soc., Dalton Trans. (2002) 3079;
(b) E. Bulak, M. Leboschka, B. Schwederski, O. Sarper, T. Varnali, J. Fiedler, F. Lissner, Th. Schleid, W. Kaim, Inorg. Chem. 46 (2007) 5562.
[10] C. Kavakli, Ph.D. Thesis, Universität Stuttgart, 2009.
[11] (a) O. Sarper, E. Bulak, W. Kaim, T. Varnali, Mol. Phys. 104 (2006) 833;
(b) O. Sarper, E. Bulak, W. Kaim, T. Varnali, J. Mol. Struct. Theochem. 773 (2006) 35.
[12] (a) U. Kölle, M. Grätzel, Angew. Chem. 99 (1987) 572. Angew. Chem., Int. Ed. Engl. 26 (1987) 568;
(b) U. Kölle, B.-S. Kang, P. Infelta, P. Compte, M. Grätzel, Chem. Ber. 122 (1989) 1869;
(c) M. Ladwig, W. Kaim, J. Organomet. Chem. 419 (1991) 233;
(d) W. Kaim, R. Reinhardt, M. Sieger, Inorg. Chem. 33 (1994) 4453;
(e) S. Fukuzumi, Eur. J. Inorg. Chem. (2008) 1351.
[13] (a) R. Ruppert, S. Hermann, E. Steckhan, J. Chem. Soc., Chem. Commun. (1988) 1150;
(b) E. Steckhan, S. Hermann, R. Ruppert, E. Dietz, M. Frede, E. Spika, Organometallics 10 (1991) 1568;
(c) D. Westerhausen, S. Hermann, W. Hummel, E. Steckhan, Angew. Chem. 104 (1992) 1496. Angew. Chem., Int. Ed. Engl. 31 (1992) 1529;
(d) E. Steckhan, S. Hermann, R. Ruppert, J. Thömmes, C. Wandrey, Angew. Chem. 102 (1990) 445. Angew. Chem., Int. Ed. Engl. 29 (1990) 388;
(e) C. Kohlmann, W. Märkle, S. Lütz, J. Mol. Catal. B: Enzym. 51 (2008) 57.
[14] W. Kaim in New Trends in Molecular Electrochemistry, A.J.L. Pombeiro, ed., Fontis Media, Lausanne, 2004, 127.
[15] W. Kaim, J. Fiedler, Chem. Soc. Rev. 38 (2009) 3373.
[16] (a) G.M. Sheldrick, SHELXL 97 Program System, University of Göttingen, Göttingen, Germany, 1997;
(b) W. Herrendorf, H. Bärnighausen, HABITUS Program, University of Karlsruhe, Karlsruhe, Germany, 1993.
[17] M.J. Frisch, G.W. Trucks, H.B. Schlegel, G.E. Scuseria, M.A. Robb, J.R. Cheeseman, J.A. Montgomery Jr., T. Vreven, K.N. Kudin, J.C. Burant, J.M. Millam, S.S. Iyengar, J. Tomasi, V. Barone, B. Mennucci, M. Cossi, G. Scalmani, N. Rega, G.A. Petersson, H. Nakatsuji, M. Hada, M. Ehara, K. Toyota, R. Fukuda, J. Hasegawa, M. Ishida, T. Nakajima, Y. Honda, O. Kitao, H. Nakai, M. Klene, X. Li, J.E. Knox, H.P. Hratchian, J.B. Cross, V. Bakken, C. Adamo, J. Jaramillo, R. Gomperts, R.E. Stratmann, O. Yazyev, A.J. Austin, R. Cammi, C. Pomelli, J.W. Ochterski, P.Y. Ayala, K. Morokuma, G.A. Voth, P. Salvador, J.J. Dannenberg, V.G. Zakrzewski, S. Dapprich, A.D. Daniels, M.C. Strain, O. Farkas, D.K. Malick, A.D. Rabuck, K. Raghavachari, J.B. Foresman, J.V. Ortiz, Q. Cui, A.G. Baboul, S. Clifford, J. Cioslowski, B.B. Stefanov, G. Liu, A. Liashenko, P. Piskorz, I. Komaromi, R.L. Martin, D.J. Fox, T. Keith, M.A. Al-Laham, C.Y. Peng, A. Nanayakkara, M. Challacombe, P.M.W. Gill, B. Johnson, W. Chen, M.W. Wong, C. Gonzalez, J.A. Pople, GAUSSIAN 03, Revision E.01, Gaussian, Inc., Wallingford, CT, 2004.